heritage

MDPI

Article

Multianalytical Non-Invasive Characterization of '*Mater Boni Consilii*' Iconography Oil Painting

Federica Valentini [1,*], Sara De Angelis [1], Livia Marinelli [2], Camilla Zaratti [2], Marcello Colapietro [3], Ombretta Tarquini [4] and Andrea Macchia [2]

[1] Chemical Sciences Technologies Department, Vergata University of Rome, Via della Ricerca Scientifica 1, 00133 Rome, Italy; saradeangelis05@gmail.com
[2] YOCOCU APS, Via T.Tasso 108, 00185 Rome, Italy; livia.marinelli@uniroma1.it (L.M.); camilla.zaratti@uniroma1.it (C.Z.); andrea.macchia@uniroma1.it (A.M.)
[3] Fondazione Roma Sapienza Piazzale Aldo Moro 5, 00185 Rome, Italy; marcello.colapietro@fondazione.uniroma1.it
[4] Institute of Crystallography, CNR, Via Salaria—km 29,300, 00015 Monterotondo, Italy; ombretta.tarquini@ic.cnr.it
* Correspondence: federica.valentini@uniroma2.it

Abstract: This paper presents the results of non-invasive diagnostic investigations performed on the canvas oil painting depicting the Marian iconography "*Mater Boni Consilii*". The painting, whose author and origin are unknown, was found in an old shop in Florence following the overflowing of the Arno River in 1966. In order to define the importance of the artwork, a multianalytical analysis was performed on the painting, using multispectral imaging, X-ray fluorescence (XRF), and Fourier Transform Infrared Spectroscopy (FTIR-ATR) for the definition of materials, with a particular focus on the identification of pigments. The results allowed for the drawing up of a color palette, composed mainly of ochre and earth pigments, cinnabar, lithopone, lead white, and ultramarine pigments. After cross-referencing the acquired information with other findings, it was possible to place the painting in the period between the end of the XIXth and the beginning of the XXth centuries.

Keywords: non-invasive characterization; diagnostic analysis; pigment identification; XRF; FTIR; indirect dating

Citation: Valentini, F.; De Angelis, S.; Marinelli, L.; Zaratti, C.; Colapietro, M.; Tarquini, O.; Macchia, A. Multianalytical Non-Invasive Characterization of '*Mater Boni Consilii*' Iconography Oil Painting. *Heritage* **2023**, *6*, 3499–3513. https://doi.org/10.3390/heritage6040186

Academic Editor: Vittoria Guglielmi

Received: 21 February 2023
Revised: 27 March 2023
Accepted: 2 April 2023
Published: 4 April 2023

1. Introduction

The flood of Florence occurred on the night between the 3rd and the 4th of November 1966, and it was a disastrous event that profoundly changed the urban layout of the city. It led to extreme damage to historical and cultural heritage, both outdoors (archaeological areas and monuments), and indoors (archives, museums, and libraries). The flood effects were serious and, in some cases, even irreversible, considering that volumes (including valuable manuscripts or rare printed works), paintings, and buildings, were covered in mud. After the disaster, many technicians, students, and young volunteers rushed to Florence, with the urge to help save and preserve the works of art defaced by the event. In this context, the painting that is the object of the present study, was found in an old shop in Via Palazzuolo (Florence).

The artwork is a devotional oil on canvas painting, sized about 35 × 28 cm and depicting the Madonna and Child (Figure 1a). Thanks to its fair state of conservation, it was possible to infer that the painting portrays the theme of *Madonna del Buon Consiglio* (*Mater Boni Consilii*). The mentioned iconography shows the half-length Virgin holding the Child to her left, with the Child tenderly wrapped around her neck while placing his hand on the rich hem of his mother's dress. Both the characters are covered by a single mantle, that descends on the shoulders of both figures, from the head of the Virgin. They also have two aureoles surrounding their heads, further surmounted by a colorful rainbow [1].

(a) (b)

Figure 1. (**a**) Oil on canvas painting depicting the theme of the *Madonna del Buon Consiglio* (*Mater Boni Consilii*), found in an old shop in Florence; (**b**) Prototype of the iconography *"Madonna del Buon Consiglio"*, preserved in the Sanctuary of Genazzano (Rome) since 1467.

Marian iconography traces its roots back to the Augustinian Sanctuary of Genazzano (Rome), where the prototype of iconography is currently preserved (Figure 1b). The worship of *Madonna del Buon Consiglio* originated in 1467, with the sudden appearance of the votive painting which hung on the walls of the Sanctuary of Genazzano. According to the historical tale, during the mid-15th century, the image was removed by an Angel from the city of Shkodra, Albania, in order to hide the holy painting from the Ottoman invaders. The iconographic image and the related cult spread quickly, achieving remarkable success, especially among the Augustinian friars. It is noteworthy that its diffusion did not develop consistently, since the cult used to shift from moments of ascent to periods of decline, during the first half of the 18th century. According to historical sources, worship reached the culmination of devotion in the last years of the 18th century, in the first part of the 19th century, and in the first half of the 20th century [1]. Generally speaking, the 18th century represents the period of the cult's greatest spread from Central Italy to the South. Concurrently, a large number of copies of the iconography (about 97,000) were distributed by devotees, as mentioned in a 1748 letter written by Andrea Bacci, canon of San Marco in Rome, and addressed to the historian De Orgio [1,2]. It is also documented that in May of 1756, the Abbot Antonio Landini arrived in the city of Florence with a copy of the icon, bringing the myth to the Church of Sant'Egidio, where we find a copy by an unknown artist, dated to 1811 (Figure 2a). On this occasion, the cult spread among the Florentine workshops, counting the numerous copies created over the period from the 18th to the 20th century [1–3].

Many of the reported paintings were realized by unknown artists, and preserved in the Florentine Dioceses (Figure 2b–d). The pictures show strong similarities despite some stylistic and chromatic variation (different colors of the mantles, the crowns of the Virgins, and the backgrounds). However, information about the spread of the cult in previous periods is still fragmentary and unclear.

The present work aims to preliminarily investigate the identity of the artwork, with specific attention paid to its dating, which implies the need to understand whether we are dealing with ancient iconography, or whether it is a late copy. In order to achieve this goal, the first analytical approach used multispectral analysis (in the UV, visible, and

infrared ranges), to distinguish the different materials comprising the painting. Ultraviolet observation and digital image acquisition allowed for identification of old and recent paint layers, overpainting, later additions, and retouches, consequently distinguishing the original from subsequent pigments and dyes, depending on the different intensities and shades of fluorescence [4–8]. The IR reflectography investigated the central layers of the painting; due to the different absorbing properties of the constitutive materials, the technique revealed the artist's working methods, showing the presence of a preparatory drawing, *pentimenti*, and retouches [4,7–10]. The second approach involved the use of X-ray fluorescence (XRF), a non-invasive technique which is able to pinpoint the elementary and qualitative composition of the employed pigments, which in turn provides useful information regarding the authenticity and indirect dating of the painting, since the periods of diffusion of certain pigments in the art market, are currently chronologically categorized [9,11,12]. Finally, Attenuated Total Reflectance Infrared Spectroscopy (FTIR-ATR) was used, to determine the nature of the varnish used [13,14].

Figure 2. Some oil on canvas depictions of the iconographic theme of *Madonna del Buon Consiglio* (*Mater Boni Consilii*), painted by unknown painters during the 18th and 20th centuries: (**a**) Madonna del Buon Consiglio, preserved in the Church of Sant'Egidio (Florence) since 1811; (**b**) Madonna del Buon Consiglio, 18th century (Diocese of Florence); (**c**) Madonna del Buon Consiglio, 19th century; and (**d**) Madonna del Buon Consiglio, painted in 1908 (Diocese of Florence).

2. Materials and Methods

The preliminary screening of the artwork was carried out by macroscopic observations and detail acquisition of the surface, using a Canon EOS 1200D digital camera with a 0.25 m/0.8 ft, 18–55 mm MACRO lens.

Visible (VIS), ultraviolet (UV), and infrared (IR) imaging were performed with a Madatec® multispectral imaging system, comprising a Samsung NX500 28.2 MP BSI CMOS camera. The UV-induced fluorescence was obtained using filters Hoya UV-IR cut 52 and Yellow 495 F-PRO MRC, with Madatec® light sources (CR230B-HP) at a wavelength of 365 nm. Additionally, 3 different visible blocking filters, at 760, 850, and 950 nm, respectively, were used for IR reflectography.

The elemental analyses were carried out by an energy-dispersive X-ray fluorescence spectroscopy (ED-XRF), using portable equipment with an X-ray generator with a W anode (EISS srl), and an experimental Peltier-cooled silicon drift detector. The XRF spectra were obtained while operating in the air at 36 kV, 350 μA, with data acquisition times of 120 s. The sampled area was approximately 2 mm in diameter. The detector resolution ranged from 140 eV to 5.9 KeV (Mn Kα). Data were processed using PyMCA software [15], and pigments were identified by consulting both Colour Lex [16], and scientific bibliographies [11,12].

Fourier Transform Infrared spectroscopy (FTIR) was performed using a Thermo Scientific Nicolet Summit Pro spectrometer with an Everest™ Diamond ATR accessory, with a spectral resolution of 4 cm^{-1}, placing the painted surface directly in contact with the

diamond of the ATR (at the paint loss in the upper left corner), investigating the spectral region between 4000–600 cm^{-1}. A total of 32 scans were performed on the sample, and the spectrum was analyzed by comparing it with databases and scientific bibliographies [13,14,17,18].

3. Results

3.1. Preliminary Observations by Visual Analysis

Viewing the acquisitions in visible light allowed the opportunity to establish the good state of conservation of the painting. It was possible to observe small signs of aging, especially on the face of the Child and on the area surrounding the lips, in which small craquelure are visible (Figure 3a). At the bottom right of the painting, there is a barely legible inscription, which is presumably linked to an acronym added by the author himself. In the final part of the inscription, the last letters (IVRI) are discreetly recognizable (Figure 3b). Along the edges of the frame there are lifts and craquelure of the paint layer (Figure 3c,d), caused by the fold of the canvas support, which occurred after the placing of the frame. Through the cracks, it is possible to catch a glimpse and distinguish the wide texture of the rough canvas, also visible at the back of the painting (Figure 3f). A small amount of paint loss is located in the upper left corner, and the frame is characterized by simple workmanship, with a thickness of 1 cm (Figure 3e). On the backside, the frame is also in a good state of conservation, and it does not show any particular signs of aging. On the top, in the central area of the frame, two small holes are visible, probably attributable to the insertion of old nails. The canvas support shows plaster residue in the lower register, near the frame ruler (Figure 3f).

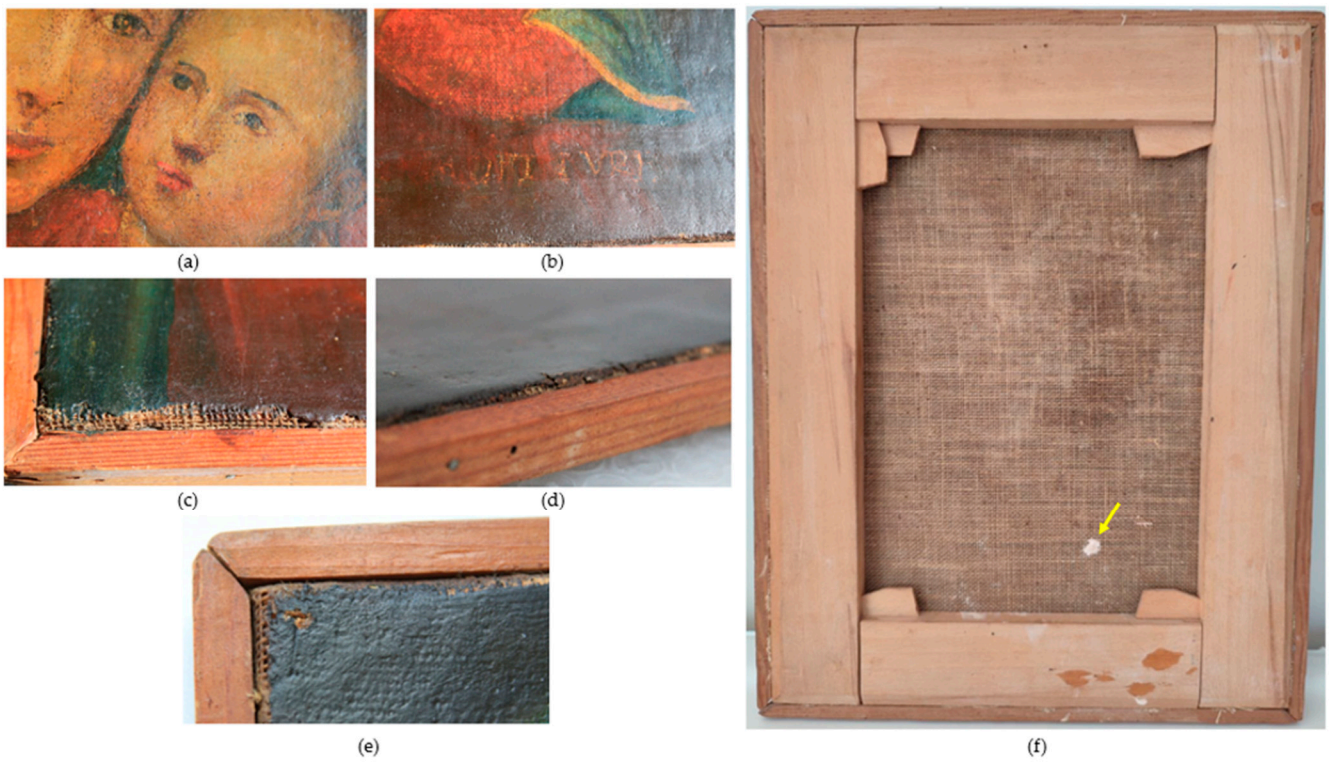

Figure 3. Macroscopic observation: (**a**) craquelure visible on the Child's lips; (**b**) inscription at the bottom right of the painting; (**c**) liftings of the paint layer; (**d**) craquelure of the paint layer; (**e**) small paint loss in the left upper corner; and (**f**) support frame (back) with plaster residue (yellow arrow).

3.2. Multispectral Imaging

The UV-induced visible fluorescence images of the painting (Figure 4) show the presence of some retouches and restoration areas, which appear as darker spots (absence of visible fluorescence) in comparison with the general green/yellow fluorescence, due to the

presence of a protective varnish. The paint additions are limited to small areas located on the faces of both the characters, on the hand of the Child, and on the crown of the Madonna (Figure 4a,b). Moreover, the uneven distribution of the varnish is noticeable, according to the presence of areas with different intensity of the green fluorescence. This last observation is more evident in the acquisitions made with the yellow filter (F-PRO MRC Yellow 495) (Figure 4b). It is possible to better distinguish areas with thinner varnish layers, which can be identified by less intense fluorescence, and areas that show an excess of varnish, identified by more intense fluorescence. As widely discussed in the scientific literature [17], different aging binders have similar fluorescence emissions.

Figure 4. UV-induced visible fluorescence: (**a**) the image shows the presence of retouches and restoration as dark details, found in the faces of both the child and the Madonna, as well as in the child's hand, and the crown of the Madonna; (**b**) inhomogeneous varnish coating probably caused by brush strokes (white arrow).

In the upper right corner, the inhomogeneous varnish coating provides information about the application process, which was probably performed using brush strokes (Figure 4b).

The IR reflectography investigation did not reveal traces of either underlying drawings made with absorbent IR material (i.e., charcoal, pencil, or black pigment brush), or traces of *pentimenti* (Figure 5). This may suggest a strong technical mastery by the artist. The background IR response showed high homogeneity and consistency, providing indicative information about the blue pigment used. In fact, based on the IR reflectography response, it is possible to assume the use of Prussian blue or ultramarine blue. According to the literature [19–21], these pigments generally show an appearance of medium gray color, that can become darker if the analyzed layer is very thick. It should be kept in mind that the pictorial layer consists of a multi-material surface, so the response could be influenced by the absorption of the outer protective films [12]. More information is provided through elemental chemical studies, which are reported in the following section.

Figure 5. IR reflectography acquisitions by using the following filters: 760 nm, 850 nm, 950 nm. No traces of underdrawings or *pentimenti* were detected.

The acquisitions made at 950 nm, made the darker areas and the brighter areas more distinguishable. It gave the impression that the artist was trying to create areas of *chiaroscuro*, by mixing the pigments with white [19,21].

Finally, in the area of the supposed acronym, a homogeneous and intense fluorescence of the varnish appeared. Such evidence allowed us to assume that the inscription was probably coeval with the realization of the painting (Figure 6b). The IR acquisitions did not allow for discernment of further letters in addition to those already identified by the first macroscopic observation (Figure 6c).

Figure 6. Details of the inscription: images acquired using Visible (**a**), UV (**b**), and IR (950 nm) (**c**); (**b**) There is a homogeneous and intense coat of varnish; (**c**) No more letters have been identified.

3.3. Elemental Analyses of Pictorial Layers (ED-XRF)

For the identification of pigments, a chemical analysis using X-ray fluorescence was carried out. As a non-destructive method, the technique was performed over 22 different points of the painting (Figure 7), in order to obtain meaningful data on the pigments, and to collect all of the different chromatic shades that define the artist's palettes [11,12].

The XRF analysis (Table 1) identified the presence of elements such as lead (Pb) and calcium (Ca) for each analyzed area, probably due to preparation of the canvas with chalk together with an *imprimitura*. This canvas was made of lead white [$2PbCO_3$ Pb(OH)], a pigment historically known as *Biacca* and which has, since ancient times, been widely used, both for the realization of primers, and for mixture in painting layers [11,12,21,22].

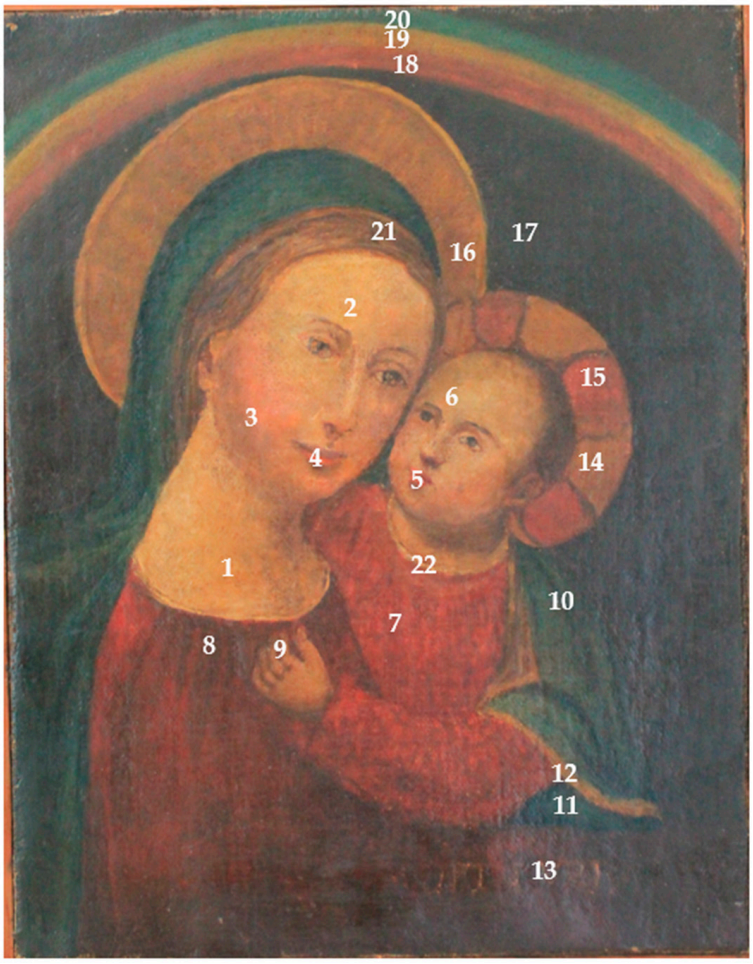

Figure 7. Mapping of the X-ray Fluorescence measuring points (1–22) in the painting. The 22 points have been chosen in order to obtain information on the different chromatic shades that define the artist's palette.

Small amounts of mercury (Hg) were detected, mainly on the cheeks and the lips of the two figures (spots 3, 4, and 5) (Figure 8a). It is reasonable to assume the use of cinnabar (natural) or vermilion (synthetic) (HgS), probably combined with white pigments, to obtain a more realistic rendering of the redness of the skin. The element which is mainly responsible for the red, green, and yellow fields, is iron (Fe), which can be related to the use of ochre (red and yellow ochre) and earth pigments (green earth) [23]. This last assumption is further confirmed by the presence of small amounts of potassium (K), titanium (Ti), and copper (Cu), which are related to impurities in the earth pigments [11,24,25]. The mentioned elements, including cinnabar, are not useful for indirect dating, due to the fact that they are widely used across all historical periods [11]. On the yellow edge of the mantle of the Madonna, and on the Child's aureole, the presence of small amounts of gold (Au) were detected, which speaks to the artist's intention of enriching and decorating the painting (Figure 8b).

Table 1. Elemental composition detected, as corresponding to the 22 investigated points. The values are expressed in percentages after being normalized to W counts.

Spot	Description	K [K]	Ca [K]	Ti [K]	Mn [K]	Fe [K]	Co [K]	Cu [L]	Zn [K]	As [K]	Sr [K]	Ba [L]	Au [L]	Hg [L]	Pb [L]
1	Neck incarnate of Madonna		3.6 ± 0.2	4.4 ± 0.5		22.2 ± 0.4		1.6 ± 0.1	30.0 ± 0.5		0.3 ± 0.1	20.5 ± 0.6			17.4 ± 0.4
2	Face incarnate of Madonna		12.0 ± 0.3	4.4 ± 0.6		8.3 ± 0.3		2.0 ± 0.2	40.5 ± 0.6		0.8 ± 0.1	28.0 ± 0.7			4.0 ± 0.2
3	Cheeks incarnate of Madonna		4.0 ± 0.2	3.6 ± 0.4		12.8 ± 0.3		1.7 ± 0.1	21.3 ± 0.4			14.7 ± 0.5		6.6 ± 0.3	35.3 ± 0.5
4	Madonna's lips		30.5 ± 0.7	2.5 ± 0.6	0.8 ± 0.2	18.5 ± 0.5		5.1 ± 0.3	20.0 ± 0.6		0.5 ± 0.2	14.6 ± 0.8		0.8 ± 0.3	6.7 ± 0.4
5	Child's lips	0.3 ± 0.1	3.3 ± 0.1	0.2 ± 0.1	1.3 ± 0.1	65.8 ± 0.6		2.0 ± 0.1	0.5 ± 0.1			1.0 ± 0.2		11.4 ± 0.3	14.5 ± 0.3
6	Face incarnate of Child		8.1 ± 0.2	3.3 ± 0.4		16.1 ± 0.3		1.6 ± 0.1	28.3 ± 0.5		0.4 ± 0.1	20.9 ± 0.6			21.4 ± 0.4
7	Child's dress	traces	9.1 ± 0.3	0.7 ± 0.2	0.7 ± 0.1	41.6 ± 0.6		2.2 ± 0.2	5.4 ± 0.3		traces	3.0. ±0.3		33.2 ± 0.5	4.0 ± 0.2
8	Madonna's dress	0.2 ± 0.1	8.9 ± 0.3	1.5 ± 0.3	0.9 ± 0.1	42.7 ± 0.6	9.7 ± 0.3	3.1 ± 0.2	16.3 ± 0.4		0.3 ± 0.1	8.4 ± 0.4		0.5 ± 0.2	7.8 ± 0.3
9	Child's index finger	0.2 ± 0.1	3.5 ± 0.2	2.6 ± 0.3	0.5 ± 0.1	37.4 ± 0.5		1.3 ± 0.1	19.5 ± 0.4		traces	13.5 ± 0.5		2.1 ± 0.2	19.6 ± 0.4
10	Green mantle (upper dx side)	0.3 ± 0.1	6.2 ± 0.2	1.2 ± 0.2	0.8 ± 0.1	50.5 ± 0.6		1.9 ± 0.1	6.7 ± 0.2			5.3 ± 0.3			27.4 ± 0.4
11	Green mantle (lower dx side)	0.4 ± 0.1	6.4 ± 0.2	0.9 ± 0.2	0.9 ± 0.1	64.2 ± 0.6		1.3 ± 0.1	4.4 ± 0.2			3.7 ± 0.3			18.2 ± 0.3
12	Mantle edge	0.2 ± 0.1	3.9 ± 0.2	0.6 ± 0.2	0.6 ± 0.1	45.9 ± 0.5		1.6 ± 0.1	4.2 ± 0.2	4.9 ± 0.4		3.2 ± 0.3	0.4 ± 0.2	1.9 ± 0.2	32.8 ± 0.6
13	Acronym	0.3 ± 0.1	5.5 ± 0.2	0.3 ± 0.1	1.2 ± 0.1	69.4 ± 0.6		1.5 ± 0.1	0.8 ± 0.1	2.7 ± 0.3		0.8 ± 0.2			17.8 ± 0.4
14	Child's aureole (yellow area)	0.3 ± 0.1	5.6 ± 0.2	1.1 ± 0.3	0.7 ± 0.1	58.7 ± 0.6		1.3 ± 0.1	5.7 ± 0.2	1.5 ± 0.3	0.2 ± 0.1	8.6 ± 0.4	0.9 ± 0.1	2.9 ± 0.2	12.9 ± 0.4
15	Child's aureole (red area)	0.4 ± 0.1	5.5 ±0.2	0.2 ± 0.1	1.0 ± 0.1	60.4 ± 0.6		1.8 ± 0.1	1.2 ± 0.2		1.2 ± 0.2	2.3 ± 0.2		17.5 ± 0.4	8.6 ± 0.3
16	Madonna's aureole		6.2 ± 0.2	1.4 ± 0.2	0.4 ± 0.1	59.6 ± 0.5		1.1 ± 0.1	7.1 ± 0.2	2.1 ± 0.2	0.2 ± 0.1	6.4 ± 0.3			15.4 ± 0.3
17	Background	0.2 ± 0.1	9.6 ± 0.3	1.2 ± 0.1	0.5 ± 0.1	43.0 ± 0.6	3.9 ± 0.2	1.6 ± 0.1	6.1 ± 0.2		traces	5.9 ± 0.3			27.9 ± 0.4
18	Rainbow (red)	0.2 ± 0.1	7.9 ± 0.2	1.3 ± 0.4	0.3 ± 0.1	35.3 ± 0.5	6.4 ± 0.3	1.4 ± 0.1	19.9 ± 0.4		0.3 ± 0.1	14.7 ± 0.5		1.8 ± 0.2	10.4 ± 0.3
19	Rainbow (yellow)		11.0 ± 0.3	1.2 ± 0.3	0.2 ± 0.1	31.5 ± 0.5	4.3 ± 0.2	1.6 ± 0.1	28.1 ± 0.5		0.4 ± 0.1	12.3 ± 0.5			9.6 ± 0.3
20	Rainbow (green)		14.5 ± 0.4	3.3 ± 0.5		21.0 ± 0.5	10.3 ± 0.3	3.0 ± 0.2	25.6 ± 0.5		0.5 ± 0.1	17.0 ± 0.6		8.9 ± 0.4	4.8 ± 0.3
21	Madonna's hair	0.3 ± 0.1	4.1 ± 0.1	0.8 ± 0.2	1.3 ± 0.1	75.0 ± 0.6		1.0 ± 0.1	4.0 ± 0.1		traces	4.7 ± 0.3		0.7 ± 0.1	8.1 ± 0.2
22	Child's collar	traces	7.3 ± 0.2	2.2 ± 0.4	0.4 ± 0.1	30.8 ± 0.5		1.7 ± 0.1	16.3 ± 0.4		0.3 ± 0.1	15.6 ± 0.5		2.3 ± 0.2	23.0 ± 0.4

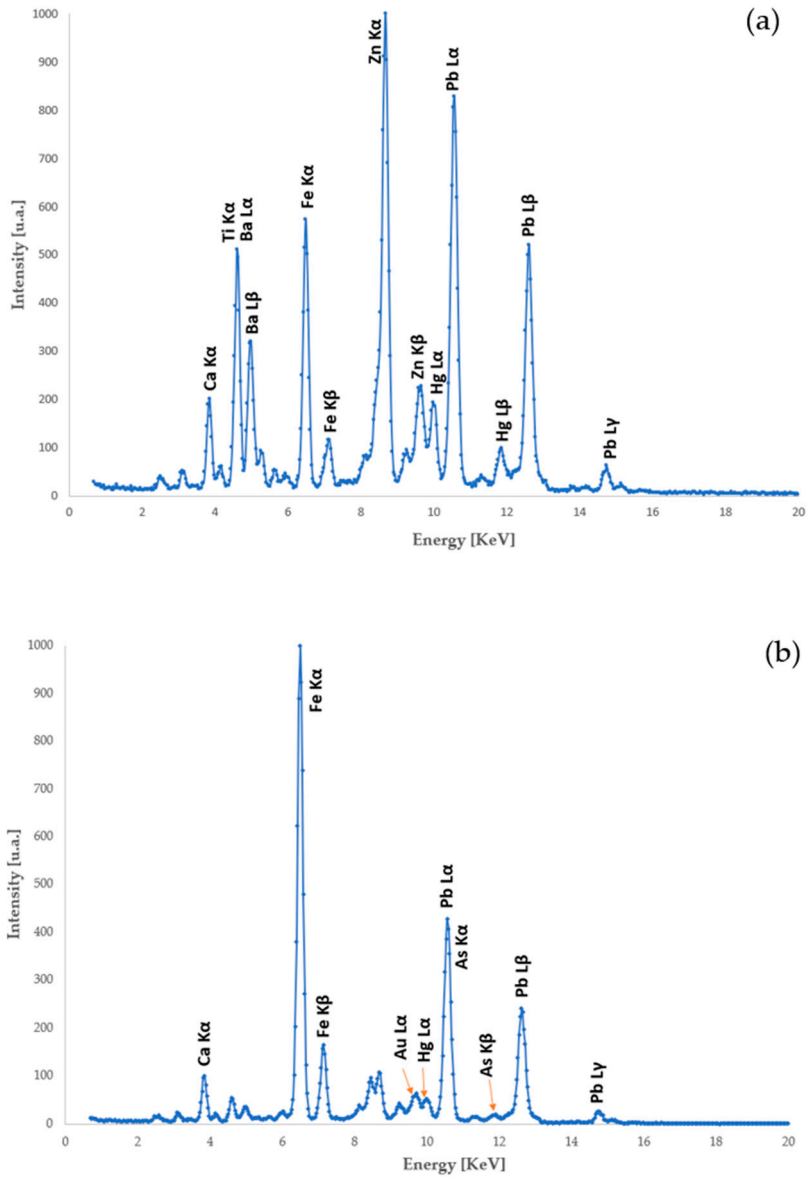

Figure 8. XRF spectra: (**a**) spot 3, cheeks incarnate of Madonna; (**b**) spot 12, mantle edge. The main peaks are marked.

The presence of lead (Pb), zinc (Zn), and barium (Ba), suggest the use of many white pigments, which were often mixed together in an effort to improve the aesthetic qualities of the white color [26]. The measurements of the incarnate (spots 1, 2, and 6) show greater intensities of the elements of zinc (Zn) and barium (Ba) than that of lead (Pb). This is connected to the choice of the artist to use a different white pigment, created by the union of Zinc white (ZnO) and *Blanc Fixe* ($BaSO_4$), or by using Lithopone ($ZnS + BaSO_4$) for the realization of the complexions. The latter is a pigment of inorganic, mineral, and synthetic origin, which is obtainable through coprecipitation, by reacting barium sulfide and zinc sulfate in such a way that the contents of the two elements are in a fixed ratio [11]. From the fixed Zn/Ba ratio found in the measurements of the incarnates (Table 2), such a balanced use is presumed, with this information being extremely important for purposes of indirect dating. In fact, Lithopone was introduced and used as a substitute for Lead white, following the discovery, in 1874, of its toxicity [11,24].

Table 2. Zinc (Zn) and barium (Ba) compositions detected in the 22 investigated points, and their respective ratios (Zn/Ba).

Spot	Description	Zn [K]	Ba [L]	Zn/Ba Ratio
1	Neck incarnate of Madonna	30.0 ± 0.5	20.5 ± 0.6	1.46 ± 0.07
2	Face incarnate of Madonna	40.5 ± 0.6	28.0 ± 0.7	1.45 ± 0.06
3	Cheeks incarnate of Madonna	21.3 ± 0.4	14.7 ± 0.5	1.44 ± 0.08
4	Madonna's lips	20.0 ± 0.6	14.6 ± 0.8	1.36 ± 0.12
5	Child's lips	0.5 ± 0.1	1.0 ± 0.2	0.50 ± 0.20
6	Face incarnate of Child	28.3 ± 0.5	20.9 ± 0.6	1.35 ± 0.06
7	Child's dress	5.4 ± 0.3	3.0. ±0.3	1.8 ± 0.28
8	Madonna's dress	16.3 ± 0.4	8.4 ± 0.4	1.94 ± 0.14
9	Child's index finger	19.5 ± 0.4	13.5 ± 0.5	1.44 ± 0.08
10	Green mantle (upper dx side)	6.7 ± 0.2	5.3 ± 0.3	1.20 ± 0.11
11	Green mantle (lower dx side)	4.4 ± 0.2	3.7 ± 0.3	1.18 ± 0.15
12	Mantle edge	4.2 ± 0.2	3.2 ± 0.3	1.31 ± 0.19
13	Acronym	0.8 ± 0.1	0.8 ± 0.2	1.00 ± 0.38
14	Child's aureole (yellow area)	5.7 ± 0.2	8.6 ± 0.4	0.66 ± 0.05
15	Child's aureole (red area)	1.2 ± 0.2	2.3 ± 0.2	0.52 ± 0.13
16	Madonna's aureole	7.1 ± 0.2	6.4 ± 0.3	1.10 ± 0.08
17	Background	6.1 ± 0.2	5.9 ± 0.3	1.03 ± 0.09
18	Rainbow (red)	19.9 ± 0.4	14.7 ± 0.5	1.35 ± 0.07
19	Rainbow (yellow)	28.1 ± 0.5	12.3 ± 0.5	9.60 ± 0.13
20	Rainbow (green)	25.6 ± 0.5	17.0 ± 0.6	4.80 ± 0.08
21	Madonna's hair	4.0 ± 0.1	4.7 ± 0.3	8.10 ± 0.08
22	Child's collar	16.3 ± 0.4	15.6 ± 0.5	23.0 ± 0.10

3.4. FTIR-ATR Spectroscopy

XRF analysis was found inadequate for the identification of the blue pigment, due to the limitations of the instrument. However, the absence of the characteristic peaks referable to other historically-used blue pigments, allows us to hypothesize the use of either Prussian blue ($Fe_4[Fe(CN)_6]\cdot nH_2O$) or ultramarine blue ($Na_8Al_6Si_6O_{24}S_4$) [11,20]. More observations on this subject are provided by the only FTIR analysis undertaken in this study (Figure 9, Table 3).

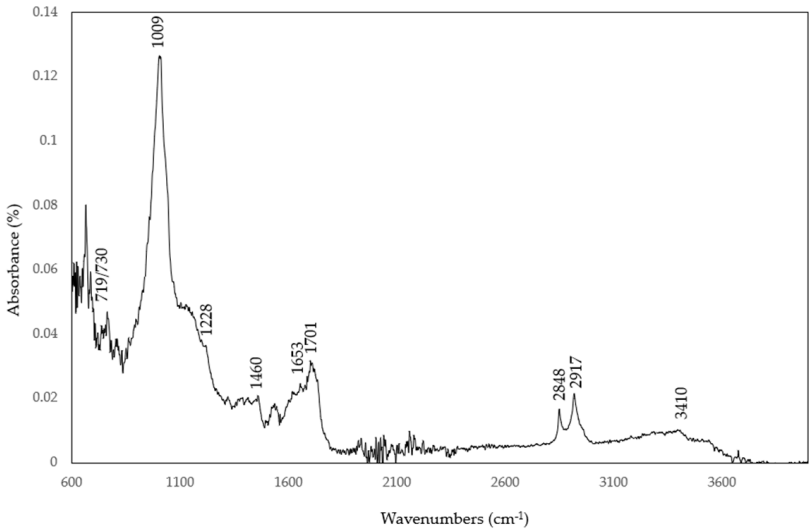

Figure 9. FTIR-ATR spectra collected in the blue background of the painting, on the paint loss (in the upper left corner).

Table 3. Summary of the absorption bands and the characteristic peaks collected using FTIR-ATR spectroscopy.

Wavenumber (cm^{-1})	Functional Group
2917	C-H stretch
2848	C-H stretch
1701	C=O stretch
1460	CH_2 bend
1653	C=C stretch
1228	C-O stretch
730/720	CH_2 rocking
1009	Si-O stretch

The ATR spectrum obtained shows an intense band at ~950–1100 cm^{-1}, related to the characteristic bands of silicates, in particular bands of ≀(Si-O-Si)™ and (Si-O-Al), probably linked with the constitutive units of the lazurite [27], which is the main component of the ornamental stone from which the ultramarine blue pigment is produced. The absence of the typical bands related to the asymmetric stretching of the C≡N group at ~2090 cm^{-1}, in agreement with the IRUG database [28,29], allows us to exclude the use of the Prussian Blue, a pigment composed of ferric ferrocyanide ($Fe_4[Fe(CN)_6]\cdot nH_2O$). From those data, we assume the use of ultramarine blue ($Na_8Al_6Si_6O_{24}S_4$), for the realization of the background.

Finally, it was possible to recognize the nature of the varnish by using FTIR analysis. The characteristic absorbances of natural resin were clearly distinguished: bands at 2917 and 2848 cm^{-1} can generally be attributed to the C-H stretching; the band centred at ~1701 cm^{-1} can be related to C=O stretching of carboxylic group of fatty acid and esters; the band at ~1460 cm^{-1} is related to the bending of the CH_2 groups and the asymmetric bending of the CH_3 groups; the band at 1653 cm^{-1} is due to C=C stretching; the band at ~1230 cm^{-1} is related to C-O stretching; and the band at ~3410 cm^{-1} is due to O-H stretching [8,14,18,30–37]. According to the literature [8,14,18,30–34], we can hypothesize the presence of shellac, which is a sesquiterpenic resin of animal origin that is secreted by an insect (Laccifer lacca) that infests the trees on which the resin is deposited. Historically speaking, shellac was mainly used not only for wooden furniture, but also as a varnish for paintings, although this application remained unknown in Europe until the 16th century [30]. Furthermore, sometimes it was mixed with other resins or waxes; in fact, the presence in the FTIR spectrum of a double band at ~730/720 cm^{-1}, is probably due to the accompanying shellac wax [18].

4. Discussion

The combined use of different analytical techniques, allowed us to study the painter's palettes (Table 4), which are apparently composed of a few pigments, primarily based on green earths, yellows, and red ochres. The use of raw materials as artistic pigments started in prehistoric times, following which their usage spread, due to low cost and ready availability [23]. Furthermore, natural-based colored pigments were often mixed with white powders, which were used from the second half of the XIX century onwards, according to the analysis carried out in the present study. In particular, the presence of zinc and barium, with traces of titanium, reveals the use of Lithopone, which, as mentioned above, was introduced in 1874 [11,24].

As a matter of fact, white pigments are the most widely employed pictorial materials, but also the most replaced compounds, from the second half of 19th century and the first half of the 20th century [26]. The substitution was carried out due to the awareness of the toxicity of white Lead [26,27], which had been used daily until that time. The changeover started during the Industrial Revolution, and immediately after the Second World War [38–41], white Lead was permanently abandoned. In the 1920s, further white pigments were introduced, including Lithopone (1920–1940), and white mixed from zinc

and titanium (1940–1960). Both zinc and titanium will be replaced by modern titanium white (1960) [42,43], which features excellent covering power and wider availability [26].

Table 4. Summary of the artist's palettes as obtained by XRF analysis, and their historical periods of use.

Colour	Spots of Analysis	Identification	History of Use
White	1; 2; 6	Lithopone	XIX century
Red	8; 7; 15; 18	Red ochres	Prehistory
Yellow	12; 14; 16; 19; 22	Yellow ochres	Prehistory
Green	10; 11; 20	Green earth	XIV century
Brown	21	Ochres	Prehistory
Red of incarnate	3; 4; 5	Cinnabar or Vermilion	XVI century
Blue	17	Ultramarine blue	XIV century.

The crucial element of the devotional paintings is the use of pigments with symbolic chromatism: the ultramarine blue (lapis lazuli) was used to indicate spirituality, the gold was related to sovereignty, and the red cinnabar denoted sacrifice [11]. This symbolic use of color also applies to the present study. Using a multianalytical approach, it was possible to detect the use of ultramarine for the background, and the application of cinnabar for the carnation of the two figures. According to technical sources, ultramarine blue was widely used in Europe between the XIVth and XVth centuries. Due to its high price, it was gradually replaced with cheaper alternatives, until artificial ultramarine was finally synthesized, in 1828 [44]. Since natural and artificial ultramarine blue have similar chemical compositions and properties, discerning between the two is difficult, but still possible. Further studies on the application of Raman spectroscopy, and more invasive analyses, i.e., optical techniques or scanning electron microscopy, could better clarify this aspect.

A similar issue is often found in the case of cinnabar. Its primary natural form is red mineral mercury sulfide powder, whose use is attested to in antiquity. In medieval Europe, the artificial alternative began to be produced under the name *vermilion* [45,46]. Due to their compositional similarities, it is not always possible to distinguish natural cinnabar (*cinnabar*) from synthetic (*vermilion*), using analytical techniques. Despite that, the electrochemical characteristics of impurities involved in the formation process could provide information that is helpful for resolving this issue [46–48].

However, the presence of Lithopone in the artist's palette provides information that assists in answering our question. Therefore, we are able to establish a terminus post quem (1874), determining the modern production. From these observations it is possible to outline the identity of the artwork, and to date it back to a temporal range between the 19th and 20th centuries. To conclude this issue, the painting can be defined as a copy.

5. Conclusions

A non-invasive diagnostic campaign was carried out, with the aim of obtaining information useful to determining the date of the artwork. Combining different scientific techniques (multispectral imaging, XRF, and FTIR-ATR) made it possible to understand the creative process of the work, the pigments that characterized the artist's palettes, and the state of conservation of the painting. Imaging investigations revealed a good state of preservation, including the presence of retouches and restorations carried out in small areas of the painting (faces of the two figures), and the absence of an underdrawing, suggesting a freedom of execution by the artist. The palettes used by the artist consisted mainly of ochres (red and yellow ochre), earth pigments (green earth), ultramarine blue (which was used for the realization of the background), and white Lead, which suggests the presence of a preparatory layer based on *biacca* and gypsum. For the incarnate, the presence of Lithopone confers the terminus post quem of the work, considering that production of it began in 1874. Therefore, it is possible to classify the artwork as one of the copies of classical iconography, and to place it in a time range between the 19th and 20th centuries.

FTIR spectroscopic analysis allowed for determination of the nature of the varnish applied, which consisted of shellac and accompanying waxes.

These results could be helpful for conservators, especially for those planning a correct intervention of conservation and restoration, and for solving attribution issues that in this case are unresolved. In fact, it was not possible to identify the acronym at the bottom of the painting, but a future study of historical-iconographic type, could clarify the issue.

Author Contributions: Conceptualization, F.V. and A.M.; methodology, F.V. and M.C.; formal analysis, S.D.A., L.M., O.T.; investigation, S.D.A., O.T., C.Z.; data curation, F.V., S.D.A.; writing—original draft preparation, S.D.A., F.V.; writing—review and editing, F.V., S.D.A.; supervision, A.M. and F.V. All authors have read and agreed to the published version of the manuscript.

Funding: This research received no external funding.

Data Availability Statement: Data is contained within the article.

Conflicts of Interest: The authors declare no conflict of interest.

References

1. Delbianco, V. La Madonna del Buon Consiglio. Storia e Fortuna di Un'iconografia Mariana. Il Caso del Trentino. 2016. Available online: https://www.academia.edu (accessed on 4 October 2022).
2. De Orgio, A.M. *Istoriche Notizie Della Prodigiosa Apparizione Dell'immagine di Maria Santissima del Buon Consiglio Nella Chiesa de'Padri Agostiniani di Genazzano*; Stamperia di S. Michele per Ottavio Puccinelli: Rome, Italy, 1748.
3. BeWeB-Beni Ecclesiastici in Web CEI-Ufficio Nazionale per i Beni Culturali Ecclesiastici e L'edilizia di Culto. Available online: https://www.beweb.chiesacattolica.it/UI/page.jsp?action=ricerca%2Frisultati&view=griglia&locale=it&ordine=&ambito=CEIOA&liberadescr=Madonna+del+Buon+consiglio&liberaluogo=Firenze (accessed on 4 October 2022).
4. Pelagotti, A.; Del Mastio, A.; De Rosa, A.; Piva, A. Multispectral imaging of paintings. *IEEE Signal Process. Mag.* **2008**, *25*, 27–36. [CrossRef]
5. Pelagotti, A.; Pezzati, L.; Bevilacqua, N.; Vascotto, V.; Reillon, V.; Daffara, C. A Study of UV Fluorescence Emission of Painting Materials. In Proceedings of the 8th International Conference on Non-Destructive Testing and Microanalysis for the Diagnostics and Conservation of the Cultural and Environmental Heritage, Lecce, Italy, 15–19 May 2005.
6. Macovaz, V. Indagini e diagnostica fotografica per i Beni Culturali. In *Relazione Tecnica*; Diagnostica per i BBCC: Trieste, Italy, 2016.
7. Bitossi, G.; Giorgi, R.; Mauro, M.; Salvadori, B.; Dei, L. Spectroscopic Techniques in Cultural Heritage Conservation: A Survey. *Appl. Spectrosc. Rev.* **2005**, *40*, 187–228. [CrossRef]
8. Macchia, A.; Aureli, H.; Colasanti, I.A.; Rivaroli, L.; Tarquini, O.; Sabatini, M.; Dattanasio, M.; Pantoja Munoz, L.; Colapietro, M.; La Russa, M.F. IN SITU DIAGNOSTIC ANALYSIS OF THE SECOND HALF OF XVIII CENTURY "MORTE DI SANT'ORSOLA" PANEL PAINTING COMING FROM CHIESA DEI SANTI LEONARDO E ERASMO ROCCAGORGA (LT, ITALY). *Int. J. Conserv. Sci.* **2021**, *12*, 1377–1390.
9. Saladino, M.L.; Ridolfi, S.; Carocci, I.; Martino, D.C.; Lombardo, R.; Spinella, A.; Traina, G.; Caponetti, E. A multianalytical non-invasive and micro-invasive approach to canvas oil paintings. General considerations from a specific case. *Microchem. J.* **2017**, *133*, 607–613. [CrossRef]
10. Bottoli, A.; Marchiafava, V. *Colore e Colorimetria. Contributi Multidisciplinari. Vol. XV A.*; Gruppo del Colore—Associazione Italiana Colore: Milan, Italy, 2019.
11. Bevilacqua, N.; Borgioli, L.; Adrover, G.I. *I Pigmenti Nell'arte. Dalla Preistoria Alla Rivoluzione Industriale*; Il Prato: Nikko, Japan, 2019.
12. Seccaroni, C.; Moioli, P. *Fluorescenza X. Prontuario per L'analisi XRF Portatile Applica a Superfici Policrome*; Nardini Editore: Florence, Italy, 2004.
13. Mailunas, R.J.; Bensten, J.G.; Steinberg, A. Analysis of aged paint binders by FTIR Spectroscopy. *Stud. Conserv.* **1990**, *35*, 33–51.
14. Silverstein, R.M.; Webster, F.X.; Kiemle, D.J. *Identificazione Spettrometrica di Composti Organici. Casa Editrice Ambrosiana Distribuzione Esclusiva Zanichelli*; Wiley: Hoboken, NJ, USA, 2016.
15. Solé, V.A.; Papillon, E.; Cotte, M.; Walter, P.; Susini, J. A multiplatform code for the analysis of energy-dispersive X-ray fluorescence spectra. *Spectrochim. Acta Part B* **2007**, *62*, 63–68. [CrossRef]
16. ColourLex. Available online: https://colourlex.com/ (accessed on 5 November 2022).
17. Longoni, M.; Cacciola, E.S.; Bruni, S. UV-Excited Fluorescence as a Basis for the In-Situ Identification of Natural Binders in Historical Painting: A critical Study on Model Samples. *Chemosensors* **2022**, *10*, 256. [CrossRef]
18. Derrick, M.; Stilik, D.; Landry, J.M. *Infrared Spectroscopy in Conservation Science (Scientific Tools for Conservation)*; The Getty Conservation Institute: Los Angeles, CA, USA, 1999.

19. Raïch, M.; Artoni, P.; Herrero, M.A.; La Bella, A.; Ricci, M.L.; Hernàndez, A. Riconoscere dal colore. Pigmenti e coloranti dell'età moderna nell'analisi multibanda dei dipinti: Uno strumento visivo per gli storici dell'arte e i conservatori. In *Colore e Colorimetria. Contributi Multidisciplinari*; Bottoli, A., Marchiafava, V., Eds.; Gruppo del Colore-Associazione Italiana del Colore: Milano, Italy, 2019; Volume XV, pp. 120–127.
20. Daffara, C.; Fontana, R. Multispectral Infrared Reflectography to Differentiate Features in Paintings. *Microsc. Microanal.* **2011**, *17*, 691–695. [CrossRef]
21. Poldi, G.; Villa, G.C.F. *Dalla Conservazione Alla Storia Dell'arte-Riflettografia e Analisi non Invasive per lo Studio dei Dipinti*; Edizioni Della Normale: Pisa, Italy, 2006; pp. 91–97.
22. Lorusso, S.; Vandini, M.; Matteucci, C.; Tumidei, S.; Campanella, L. Anamnesi storica ed indagine diagnostica del dipinto ad olio su tavola "Madonna con bambino e Santi Girolamano e Caterina da Siena" attribuibile a Domenica Baccafumi (1486–1551). *Quad. Di Sci. Della Conserv.* **2003**, 47–68.
23. Hradil, D.; Grygar, T.; Hradilová, J.; BezdičKa, P. Clay and iron oxide pigments in the history of painting. *Appl. Clay Sci.* **2003**, *22*, 223–236. [CrossRef]
24. Picollo, M.; Bacci, M.; Magrini, D.; Radicati, B.; Trumpy, G.; Tsukada, M.; Kunzelman, D. Modern White Pigment: Their Identification By Means of Noninvasive Ultraviolet, Visible, and Infrared Fiber Optic Reflectance Spectroscopy. In *Modern Paints Uncovered: Proceedings from the Modern Paints Uncovered Symposium, Tate Modern, London, UK, 16–19 May 2006*; Learner, T.J.S., Smithen, P., Krueger, J.W., Schilling, M.R., Eds.; Getty Conservation Institute: London, UK, 2006; pp. 118–128.
25. Bracci, S.; Giachi, G.; Liverani, P.; Pallecchi, P.; Paolucci, F. *Polychromy in Ancient Sculpture and Architecture*; Casa Editrice Sillabe S.r.l.: Livorno, Italy, 2018.
26. Pronti, L.; Felici, A.C.; Ménager, M.; Vieillescazes, C.; Piacentini, M. Spectral Behavior of White Pigment Mixtures Using Reflectance, Ultraviolet-Fluorescence Spectroscopy, and Multispectral Imaging. *Appl. Spectrosc.* **2017**, *71*, 2616–2625. [CrossRef]
27. Gettens, R.J.; Kühn, H.; Chase, W.T. Lead White. In *Artists' Pigments. A Handbook of Their History and Characteristics*; Roy, A., Ed.; Oxford University Press: London, UK, 1993; Volume 2.
28. Infrared and Raman Users Group Spectral Database (IRUG Database). Available online: www.irug.org (accessed on 13 December 2022).
29. Rampazzi, L.; Brunello, V.; Corti, C.; Lissoni, E. Non-invasive techniques for revealing the palette of the Romantic painter Francesco Hayez. *Spectrochim. Acta Part A Mol. Biomol. Spectrosc.* **2017**, *176*, 142–154. [CrossRef]
30. Derry, J. *Investigationg Shellac: Documenting the Process, Defining the Product: A Study on the Processiong Methods of Shellac, and the Analysis of Selected Physical and Chemical Characteristics*; The Institute of Archeology, Conservation and History: Oslo, Norway, 2012.
31. Masae, M.; Pitsuwan, P.; Sikong, L.; Kooptarnond, K.; Kongsong, P.; Phoempoon, P. Termo-physical characterization of paraffin and beeswax on cotton fabric. *Thammasat Int. J. Sci. Technol.* **2014**, *19*, 69–77.
32. Svečnjak, L.; Baranović, G.; Vinceković, M.; Prđun, S.; Bubalo, D.; Gajger, I.T. An approach for routine analytical detection of beeswax adulteration using ftir-atr spectroscopy. *J. Apic. Sci.* **2015**, *59*, 37–49. [CrossRef]
33. Hepburn, H.R. Composition and Synthesis of Beeswax. In *Honeybees and Wax*; Springer: Berlin/Heidelberg, Germany, 1986; pp. 44–56.
34. Macchia, A.; Biribicchi, C.; Carnazza, P.; Montorsi, S.; Sangiorgi, N.; Demasi, G.; Prestileo, F.; Cerafogli, E.; Colasanti, I.A.; Aureli, H.; et al. Multi-Analytical Investigation of the Oil Painting "Il Venditore di Cerini" by Antonio Mancini and Definition of the Best Green Cleaning Treatment. *Sustainability* **2022**, *14*, 3972. [CrossRef]
35. Obradovic, J.; Petibon, F.; Fardim, P. Preparation and Characterisation of Cellulose-Shellac Biocomposites. *BioResources* **2017**, *12*, 1943–1959. [CrossRef]
36. Abdel-Ghani, M. Dating a Coptic Icon of Anonymous Painter by Spectroscopic Study of Pigment Palette. *Mediterr. Archaeol. Archaeom.* **2015**, *15*, 23–37.
37. Sarkar, P.C.; Kumar, K.K. An investigation into the different forms of lac resin using FT-IR and diffuse reflectance spectroscopy. *Pigment. Resin Technol.* **2001**, *30*, 25–33. [CrossRef]
38. Guttens, R.J.; Stout, G.L. *Painting Materials: A Short Encyclopedia*; Dover Publications: Mineola, NY, USA, 1966; pp. 31–35.
39. Bacci, M.; Picollo, M.; Trumpy, G.; Tsukada, M.; Kunzelman, D. Non-Invasive Identification of White Pigments on 20th Century Oil Piantings by Using Fiber Optic Reflectance Spectroscopy. *J. Am. Inst. Conserv.* **2007**, *46*, 27–37. [CrossRef]
40. Brunner, H. Pitture. In *Storia Della Tecnologia*; Singer, C., Holmyard, A.J., Hall, A.R., Williams, T., Eds.; Bollati Boringhieri: Turin, Italy, 1982; Volume 6, pp. 617–631.
41. Laver, M. Titanium white. In *Artists' Pigments: A Handbook of Their History and Characteristics*; West FitzHugh, E., Ed.; National gallery of Art, Archetype Publications: London, UK, 1997; Volume 3, pp. 295–355.
42. Van Driel, B.A. *White, Friends or Foe? Understanding and Predicting Photocatalytic Degradation of Modern Oil Paintings*; Delft University of Technology: Delft, The Netherlands, 2018. [CrossRef]
43. Barnett, J.R.; Miller, S.; Pearce, E. Colour and art: A brief history of pigments. *Opt. Laser Technol.* **2006**, *38*, 445–453. [CrossRef]
44. Osticioli, I.; Mendes, N.F.C.; Nervin, A.; Gil, F.P.S.C.; Becucci, M.; Castellucci, E. Analysis of natural and artificial ultramarine blue pigments using laser induced beakdown and pulsed Raman spectroscopy, statistical analysis a light microscopy. *Spectrochim. Acta Part A* **2009**, *73*, 525–531. [CrossRef] [PubMed]
45. Miguel, C.; Pinto, J.V.; Clarke, M.; Melo, M.J. The alchemy of red mercury sulphide: The production of vermilion for medieval art. *Dyes Pigment.* **2014**, *102*, 210–217. [CrossRef]

46. Gettens, R.J.; Feller, R.L.; Chase, W.T. Vermilion and Cinnabar. *Stud. Conserv.* **1972**, *17*, 45–69.
47. Nöller, R. Cinnabar reviewed: Characterization of red pigment and its reactions. *Stud. Conserv.* **2013**, *60*, 79–87. [CrossRef]
48. Edwards, H.G.M. Historical Pigments: A Survey of Analytical Chemical Archaemetric Usage and Terminology for Forensic Art Analysis. In *Encyclopedia of Analytical Chemistry: Applications, Theory and Instrumentation*; Wiley: Hoboken, NJ, USA, 2015. [CrossRef]